LA-UR- 95-2367

Conf-950750--14

Los Alamos National Laboratory is operated by the University of California for the United States Department of Energy under contract W-7405-ENG-36.

TITLE: RESULTS OF RUSSIAN/US HIGH PERFORMANCE DEMG EXPERIMENT

AUTHOR(S): A. M. Büyko, N. P. Bidylo, V. K. Chernyshev, V. A. Demidov
S. F. Garanin, V. N. Kostyukov, A. A. Kulagin, A. I. Kuzyaev
A. B. Mezhevov, V. N. Mokhov, E. S. Pavlovskiy, A. A. Petrukhin
V. B. Yakubov, B. T. Yegorychev, (All Russian Scientific Research Institute of Experimental Physics)
J. W. Canada, C. A. Ekdahl, J. H. Goforth, J. C. King, I. R. Lindemuth
R. E. Reinovsky, P. Rodriguez, R. C. Smith, L. R. Veeser, S. M. Younger

SUBMITTED TO: 10TH IEEE INTERNATIONAL PULSED POWER CONFERENCE
JULY 10-13, 1995

Los Alamos National Laboratory
Los Alamos, New Mexico 87545

FORM NO 836 R4
ST NO 2629 5/81

DISCLAIMER

RESULTS OF RUSSIAN/US HIGH PERFORMANCE DEMG EXPERIMENT*

A. M. Buyko, N. P. Bidylo, V. K. Chernyshev, V. A. Demidov, S. F. Garanin,
V. N. Kostyukov, A. A. Kulagin, A. I. Kuzyaev, A. B. Mezhevov, V. N. Mokhov,
E. S. Pavlovskiy, A. A. Petrukhin, V. B. Yakubov, B. T. Yegorychev

All Russian Scientific Research Institute of Experimental Physics
Arzamas-16, Nizhni Novgorod, Russia

J. W. Canada, C. A. Ekdahl, J. H. Goforth, J. C. King, I. R.Lindemuth,
R. E. Reinovsky, P. Rodriguez, R. C. Smith, L. R. Veeser, S. M. Younger

Los Alamos National Laboratory
Los Alamos New Mexico, USA

ABSTRACT

In November 1992, the All Russian Scientific Research Institute of Experimental Physics (VNIIEF), Arzamas-16, Russia and the Los Alamos National Laboratory, Los Alamos NM, USA embarked on a historic effort to conduct a joint explosive pulse-power experiment. With the concurrence of the Ministry of Atomic Energy (Russia) and the Department of Energy (USA), the two laboratories entered into a Laboratory-to-Laboratory collaboration in the areas of very high energy pulse power and ultrahigh magnetic fields in order to explore problems of mutual scientific interest. The first experiment was an explosively powered, fast, high-current pulse-power experiment. The experiment employed a flux compressor, inductive store, and opening switch to demonstrate the feasibility of supplying many megajoules of electrical energy on microsecond time scales, to high energy density physics experiments. The experiment was successfully conducted in Arzamas-16 on September 22, 1993.

I. SYSTEM DESCRIPTION

The key element in the experiment was a Russian-designed very high current, fast flux compressor based on the Disk Electromagnetic Generator (DEMG) geometry.[1] The major components of the system are shown in Fig. 1 and included a capacitor bank, a helical explosive flux compressor, a disk explosive flux compressor, a fast electro-explosive (fuse) opening switch, an explosively operated solid dielectric load isolating closing switch, and an imploding aluminum liner driven to moderate velocities. The performance of a system combining a DEMG and fuse opening switch powering a static load had previously been reported.[2] The joint experiment was designed to extend that demonstration to a system including a dynamic load. Initial flux, about 2.9 webers, was provided from the capacitor bank to the helical preamplifier through an inductive coupling coil. The output of the helical preamplifier, about 6.6 MA, was directly connected to the input of the DEMG. A crowbar switch, designed to trap flux in the disk stage after helical operation, was included between helical and disk stages. The output current from the DEMG, peaking at about 50 MA, flowed through a cylindrical copper foil fuse located immediately outside the disk stages. The liner load was connected across the fuse opening switch through a low-inductance, coaxial, solid dielectric transmission line. The load was isolated from the DEMG circuit by a series, explosively operated, solid, dielectric closing switch. Current measurements were made by B-dot probes arranged in rings at several stations along the system. B-dot measurements were correlated with electro-optic magnetic field measurements made by Faraday rotation at two of the stations. The imploding liner, initially 3-cm radius and 2-cm tall, moved several millimeters before being vaporized by the load current that reached 20 MA in less than 1 μs. The implosion reached final velocities of about 3.1 cm/μs. Measurements of load behavior included B-dot, and fiber-optical and electrical contact pins.

* This work supported by the US Department of Energy.

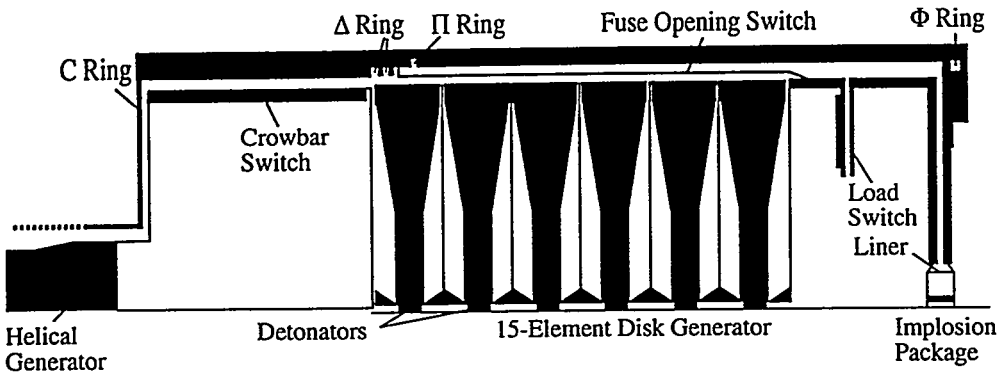

Fig. 1. Schematic view of 1993 Joint DEMG experiments.

II. DESIGN CALCULATIONS

A. Calculational Model

Using computational techniques that have previously been benchmarked against results reported in the literature,[3,4] performance of the 1993 Joint Experiment was calculated. The performance of the helical generator has been confirmed in numerous tests and was characterized simply by a range of initial currents delivered to the DEMG. The model calculates motion of the disk generator cavity walls using a modified instantaneous acceleration (Gurney) model, and magnetic pressure in the cavity. Magnetic diffusion is calculated into the walls of the disk generator and into the transmission line associated with each disk stage. Magnetic diffusion into the walls of the transmission line leading to the liner load is not calculated. The operation of the fuse opening switch is calculated using the "CONFUSE" model as previously reported.[5] The CONFUSE code models the fuse as a uniform (one-zone) ohmically heated metal layer whose expansion in one dimension is limited by moving, but uniform (one-zone) nonconducting walls. The closing switch model approximates a multichannel switch with each channel having a characteristic resistivity. Multiple channels are added in parallel with a fixed time interval between channels. The liner load is modeled as a "zero-dimensional," right-circular cylinder. Current in the liner cross-section is considered constant (the field is fully diffused) from the beginning of acceleration. Specific energy (joule/gram) is calculated in the liner material and the resistance of the liner is calculated from tabular resistivity vs. energy data. The generator, fuse, closing switch, and liner behavior is expressed as equivalent circuit elements (resistance and inductance) and the circuit elements are connected in a simple, two-loop network calculation to determine generator and load currents. In this way, load behavior is coupled to the generator performance through the current in the generator loop (and its effect on generator wall motion).

B. Parameters for the Experiment

For the 1993 Joint Experiment, we calculate the behavior of a 15-module Disk Explosive Magnetic Generator (DEMG) using an approximate cavity profile taken from previously published reports.[1] A 2-mm copper wall is employed. The cavity inductance including transmission line up to the initial radius of the fuse was specified by VNIIEF to be 11.6 NH. For the preshot calculations, the system inductance from the crowbar (which isolates the DEMG from the helical preamplifier) to the fuse was 178 NH. The system inductance consists of 175.5 NH of generator cavity and transmission line inductance, 1.82 NH of crowbar switch inductance, and 0.55 NH of additional inductance in the diagnostic sections. An initial current of 6.0 MA was assumed. For modeling purposes, an explosive composed at 70% RDX and 30% TNT was used. The detonation velocity of the mixture was taken to be 8.17 cm/μs. The density was 1.78 g/cm^3. The gurney energy is 2.78 and the detonation pressure about 310 kbar. The total mass of explosives in the DEMG was about 105 kg.

For comparison, we calculated the estimated performance of a similar 15-module generator operated into a 3.7-NH inductance representing approximately the inductance of the system transmission line up to the fuse, the crowbar switch, and the diagnostic system. Under these circumstances, the generator would be expected to produce 55 MJ of electrical energy at about 170 MA. With a fuse in the circuit, the peak generator circuit is limited to about 60 MA.

Calculations were performed using a 155-μm copper foil fuse, 1.08-m long and 1.315-m wide. The CONFUSE model predicts behavior for the fuse ranging from complete interruption (and high final resistivity) to reconduction (with relatively low final resistivity) depending on the mass of the nonconducting wall. For these calculations, a resistivity model that includes a sharp resistivity increase and good current interruption was chosen because, as will be seen in the wave forms, the sharp rise in resistivity produces substantial stress in the transmission line insulation. However, a ceiling value is imposed on the fuse resistivity corresponding to a maximum fuse resistance of about 21 mΩ. The transmission line inductance between the fuse and the initial position of the liner load was 8.55 NH. In the calculations, the load isolation switch began closing at a specified time (19.9 μs). The individual channel resistivity is 10 mΩ, and the inter channel time is 300 NS. The closing switch was supporting about 73 KV at the time that closure was initiated.

The liner load was 3 cm in radius and 2-cm high. For the baseline calculation, a liner thickness of 0.3 mm was assumed. The specific energy in the liner resulting from ohmic heating was calculated during implosion and the resistance rise due to liner heating was included in the calculation. The liner vaporized at about 21.45 μs, 1.55 μs after beginning of current flow in the load. At the time of liner vaporization, the outer radius of the liner had moved 3.2 mm or about 11 times its initial thickness. A central diagnostic package was located at a radius of 4.5 mm. The inner surface of the liner reached the diagnostic package 2.35 μs after the beginning of current in load. At this time the liner had undergone a radial compression of about 6, reached a peak velocity of about 4.2 cm/μs, and a kinetic energy of 3.2 MJ.

C. Projected Performance

The purpose of the point design was to identify the relationship between various aspects of the system's operation and to provide a quantitative basis for selection of diagnostic parameters such as sensitivity of detectors and the timing and range of recording instruments. Initial current in the calculation was 6 MA (midway between the 5.5 and 6.5 MA expected from the helical generator). Peak generator current of about 61 MA occurs at about 20.5 μs (about 600 NS after the beginning of the isolation switch closure). Peak load current was approximately 36 MA at about 21.7 μs.

Figure 2 shows the time derivative of the generator current calculated for the full experiment and on an expanded time scale. Several distinct features can be observed in the dI/dt data, including the opening of the fuse opening switch, the closing of the load isolation switch, and the implosion of the liner load. The figure includes data (dotted lines) showing the dI/dt calculated for the case where the fuse interrupts the current, and the closing switch fails to close. The figure also shows the behavior of system dI/dt for the case where current is switched into the load loop, but the liner does not implode.

The calculated fuse current peaks at about 60 MA and decreases as current is transferred to the load loop. Fuse current rises slightly at 22.25 μs as the increasing impedance of the imploding load raises the voltage imposed across the fuse whose resistance has reached it ceiling value of 21 mΩ at this time. The sharp rise in fuse resistivity predicted by CONFUSE leads to a peak in fuse voltage approaching 500 KV.

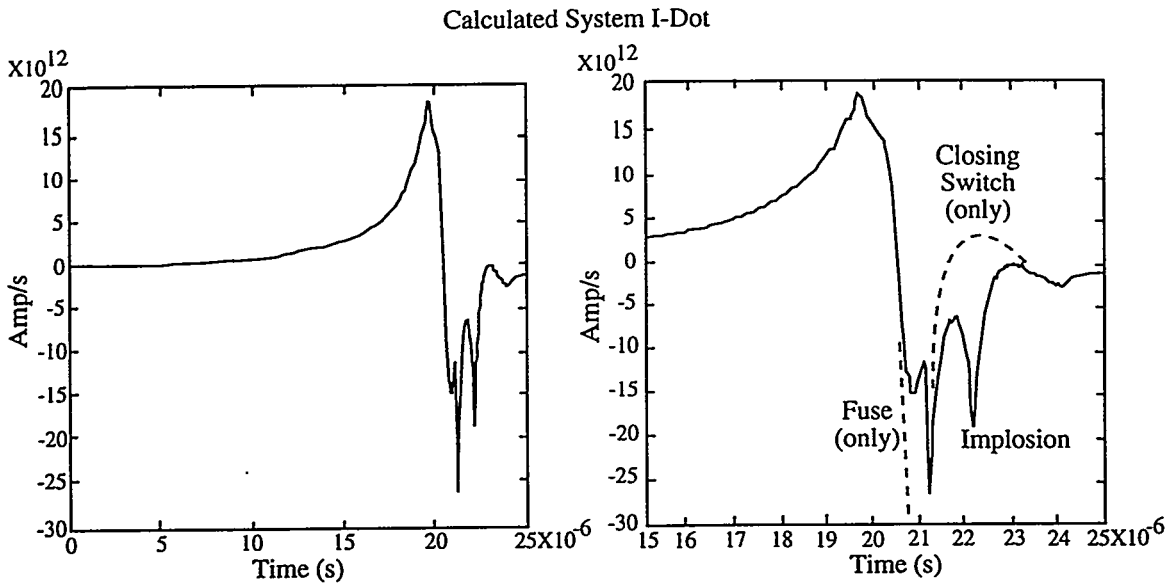

Fig. 2. The main features of the experiment are identifiable in the system dI/dt calculated from the DEMG model.

III. CAPACITOR BANK AND HELICAL FLUX COMPRESSOR OPERATION

The DEMG main energy amplifier required 1.2 webers of magnetic flux at about 6.5 MA. A helical flux compressor from the VNIIEF family of "POTOK" generators was used to provide the initial flux to the 15-element DEMG. The helical generator consisted of a wire-wound stator coil with an inner diameter of 240 mm and a length of 1200 mm. The initial inductance of the stator coil is 48 NH. The armature of the generator consists of a copper central tube. The armature tube is filled with a 21-kg charge of high explosive whose composition was 70% RDX and 30% TNT.

Initial flux is introduced into the helical flux compressor through a 28-turn coupling coil wound over the outside of the helical stator at a diameter of 280 mm and covered with epoxy. The length of the coil was 1000 mm and the coupling coefficient was about 75%. Since the coupling is significantly less than 100%, this technique introduces some inefficiency in the initial loading process but offers several advantages. First, by allowing the helical/DEMG/fuse circuit to be open prior to the operation of the helical generator, the inductive loading insures that the fuse carries no current, and hence is at room temperature when the system begins to operate. Second, the inductive coupling allows the ground connection of the capacitor bank system to be completely separate from the flux compressor ground circuit. This allows for easy isolation of the flux compressor system diagnostics from ground.

With the 1200-μF capacitor bank charged to 24 kV, the current in a coupling coil was 79.3 kA. Initial flux in a preamplifier is equal to 2.9 Wb (which was close to the planned value of 3.0 Wb). In order to prevent the flux compressor from driving substantial current and energy back into the capacitor bank circuit, the initial loading circuit is interrupted with a simple, explosively operated opening switch.

Figure 3 shows the current derivative and the current in the preamplifier circuit obtained from the average of all measuring probes located at the C ring. The design value of the preamplifier output current was 6.0 MA.[6] In the experiment, average peak current from all the probes in the helical stage was 6.6 MA. The maximum value of the current derivative averaged from all the C-Ring probes in the preamplifier was 2.1×10^{11} A/s, and the characteristic e-fold rise time of current is 28 μs. These results demonstrate that the performance of the helical flux compressors was essentially as projected.

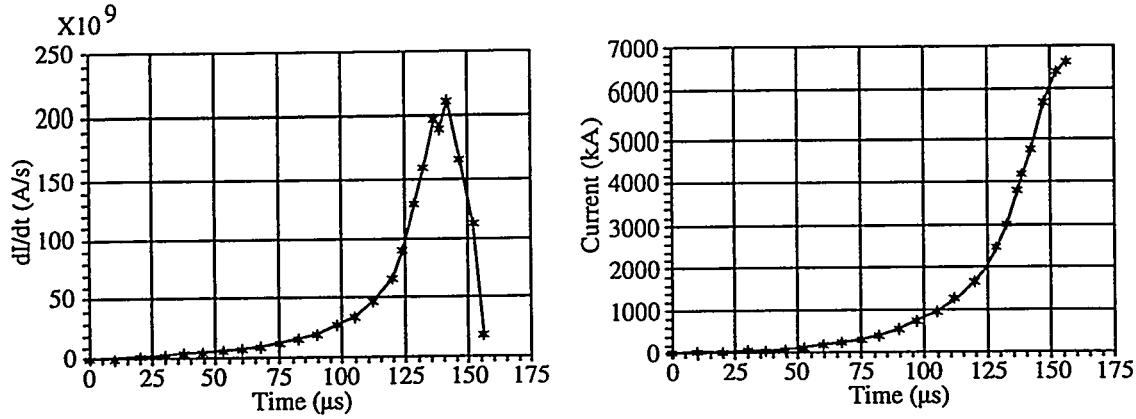

(a) (b)

Fig. 3. (a) dI/dt in helical generator, average of five probes in C Ring; (b) current in helical generator, average of five probes.

IV. PERFORMANCE OF THE DISK EXPLOSIVE MAGNETIC GENERATOR

The operation of the DEMG was recorded by probes in the Δ-Ring. For all data, time t = 0 is the firing time of the DEMG detonator firing unit. The beginning of measurable current derivative in the DEMG occurs from t = 5 to t = 6 μs. It should be noted that the observed beginning of measurable I-dot takes place somewhat after the first motion of the metallic walls in the magnetic flux compression cavities. Onset of measurable I-dot depends on the rate of magnetic flux diffusion losses in a DEMG contour, on crowbar dynamic resistance, and on differences in time of HE initiation in disk elements.

Figure 4a shows the current derivative in the DEMG as recorded by the Δ-Ring probes over the time interval t = 0 to t = 35 μs. After reaching a maximum corresponding to the time near the end of the DEMG operation when the fuse begins to rise significantly in impedance, the current derivative is seen to decrease rapidly and become negative as the fuse opens. After the brief negative excursion, I-dot again rises to approximately its former value. In contrast, Fig. 2 shows the generator I-Dot never becoming positive after the beginning of fuse operation.

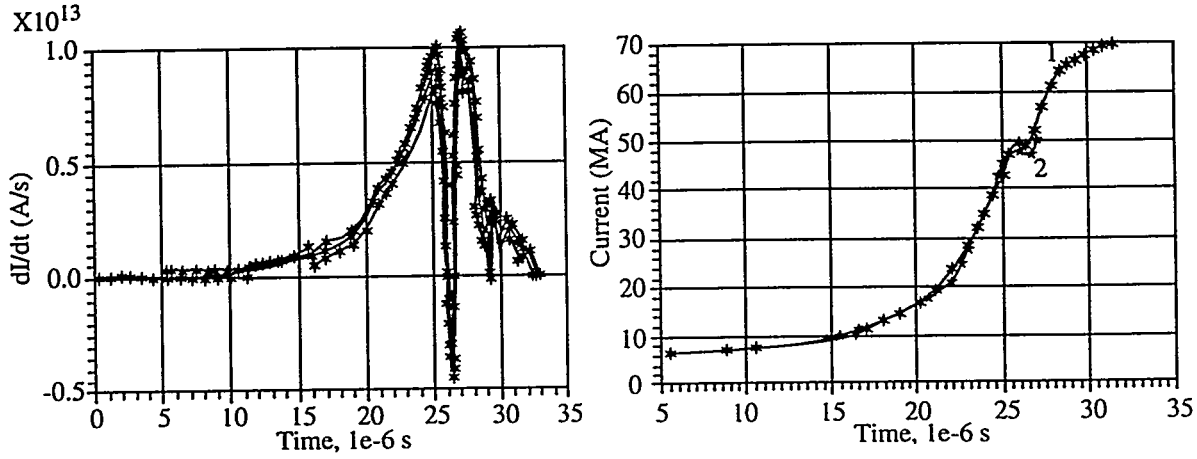

(a) (b)

Fig. 4. (a) dI/dt in DEMG from Δ probes; (b) current in DEMG from average of Δ probes.

The maximum value of a current derivative at the first positive peak is in the range from 0.82 to 1.00×10^{13} A/s for all individual probes, at the negative peak the amplitude is from 0.22 to 0.37×10^{13} A/s, and the second positive peak amplitude is from 0.9 to 1.00×10^{13} A/s. The average (over all probes) current derivative of the first positive peak was 0.9×10^{13} A/s (t = 25.2 s), the average for the negative peak associated with the operation of the fuse is 0.31×10^{13} A/s (t = 26.23 s) and the second positive peak was 0.97×10^{13} A/s. Figure 4b shows time dependence of DEMG current found from integrating the averaged current derivative. Current value at the moment of the first peak (near the end of DEMG operation) was 48.2 MA (at t = 26.0 s). The current then decreases to about 47.4 MA (at t = 26.45 s). The current in the DEMG then increases to almost to 70 MA.

V. CURRENT DELIVERY TO THE LOAD

To measure current delivery to the load, inductive probes located in probe rings at two positions downstream of the fuse were used. One of the probe rings was located at the beginning of a coaxial transmission line (Π probes) and the other ring was located at the input of a radial transmission line—the output end of the coaxial transmission line (Φ probes). Six Φ and six Π probes (twelve in all) were used in the experiment.

Figure 5 compares signals from Δ, Π, and Φ probes. Inspection of the plots shows that pulse shapes, recorded by Π and Φ probes, differ in significant ways. Both the Π and Φ probe records contain readily identifiable jumps in current derivative at about 26 μs. The discontinuities are in different directions. The records from Π probes have the jumps with a signal increase, and the records from Φ probes show a signal decrease. Furthermore, the width of the signal from Π probes is substantially wider than the width of the Φ probes. Signals from Π probes show positive values for all times of interest (indicating constantly increasing current) while signals from the Φ probes have a portion with a negative component of the current derivative (indicating a decreasing current). Taken together, the Π ring and Φ-ring data argue strongly for a partial failure of the transmission line insulation somewhere between the two rings during the time when current was being transferred to the liner load.

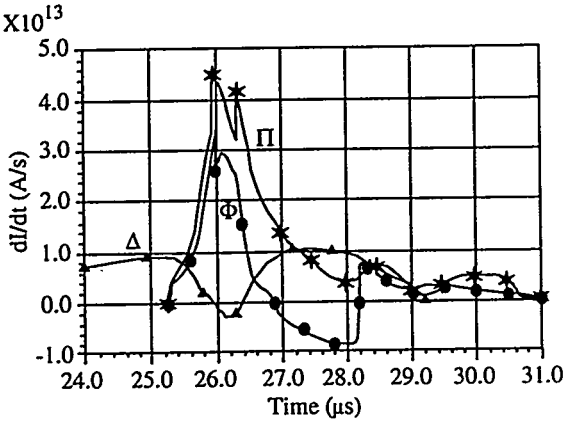

Fig. 5. Comparison of dI/dt in DEMG (Δ) with input to transmission line (Π) and at output of the transmission line (Φ).

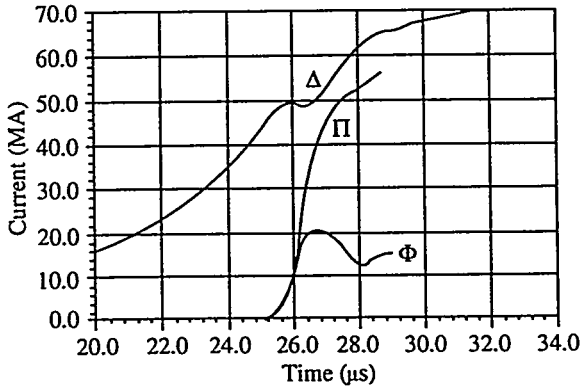

Fig. 6. Current in the DEMG (Δ), input (Π), and output (Φ) at the transmission line.

The current in the DEMG and at the Π and Φ locations is calculated from the integral of the current derivatives and are shown in Fig. 6. This plot gives averaged current curves for all Π probes and all Φ probes. It is seen from the plot that current in the load before 26 μs (the time of the first jump on a current derivative) recorded by both Π and Φ probes match. After 26 μs, the two probes disagree. Maximum current in the Π probes comes close to a current value in a disk generator. Figure 5 shows an approximate average value of the positive jump in current derivative at the Π ring is 1.4×10^{13} A/s, and the average value of the negative jump from the Φ ring is about -0.8×10^{13} A/s. Simple circuit analysis leads to the conclusion that the fuse voltage at the time of the failure was about 255 KV. The point of the

partial transmission line failure was about 3.2-NH downstream from the fuse or about 5.3-NH upstream from the load. The breakdown could be modeled as a shunt inductance of about 5.3 NH. Immediately before the failure, the transmission line was supporting about 160 KV at the failure point. After the failure, the voltage at the failure point dropped to about 115 KV.

VI. OPERATION OF THE LINER IMPLOSION (PONDERMOTIVE UNIT)

The imploding liner consists of an aluminum cylinder 3 cm in radius, 2-cm high, and 0.03-cm thick. The total mass of the imploding load is 3.05 gr. Inside the liner, a cylindrical diagnostic package is located at a radius of 4.75 mm. The package includes inductive, electrocontact, and light probes and is surrounded by a thin tantalum cylinder that protects the probes from low-density plasma thrown ahead during the vaporization of the liner. The tantalum shell is connected to the electrodes (providing a current path that allows some flux to leak through the finite resistance of the main liner) and is thin enough to be swept up by the massive liner as it implodes.

Inductive probes located inside the initial radius of the liner, but outside the Ta shell, were used to record the time derivative of magnetic field appearing inside the liner. For this purpose, four inductive probes were imbedded in the glide planes along which the liner moves at a radius of 9 mm. The time history of the magnetic field dB/dt inside the liner recorded on each of four probes expressed as a current derivative is presented in Fig. 7. Four peaks are observed in the current derivative inside the liner. The time of the first maximum, from the average of four A probes, is 26.53 μs, which corresponds to 1.29 μs from the beginning of current flow in the liner. The first maximum value is in the range from 2.2 to 3 MA/μs. Three more peaks are also observed. The averaged times for these maximum values are 27.60 s (the second maximum), 27.97 s (the third maximum), and 28.36 s (the fourth maximum), correspondingly. The time of each maximum is simultaneous on the four probes to within 100 ns.

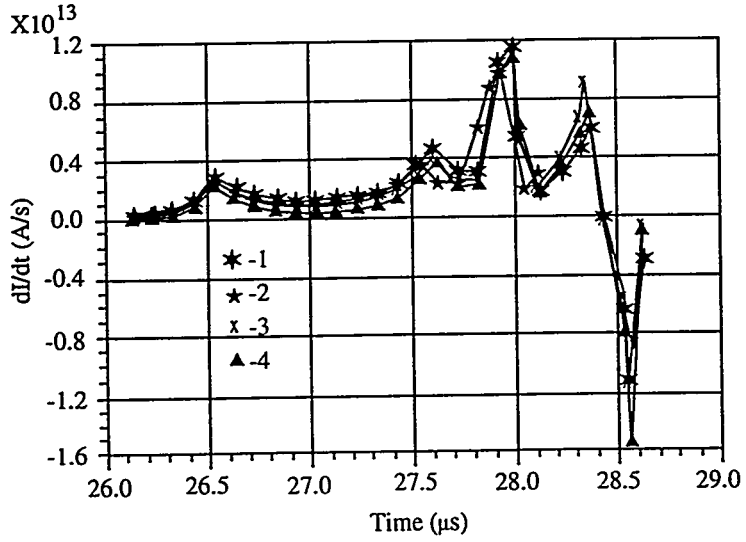

Fig. 7. Magnetic field inside liner.

The first maximum is associated with the vaporization of the liner and the time of vaporization compares reasonably well with that calculated in the model. The second peak is associated with the compression of magnetic field inside the liner. (The flux being compressed enters the space inside the liner during liner electro-explosion of the liner and is supported by current flowing in the tantalum shell surrounding the diagnostic package.) At the third peak the probe is measuring the magnetic field outside the liner after it passes the probe. In fact, the field outside the liner is substantially greater than what would be inferred from these data (equivalent dI/dt ~10^{14}) and this is attributed to a conductive layer covering the probe and partially shielding the probe from the driving field. The fourth peak is associated with the turn-around of the liner outer surface after collision with tantalum shell.

Electrocontact probes in the central diagnostic package recorded the symmetry of the imploding liner by measuring the time of arrival of the liner at the measuring unit. A total of 30 probes was employed, arranged in 6 vertical columns of 5 probes each, and was located at the radius of 4.75 mm. Data from the probes consist of time of arrival recorded digitally on an array of time interval meters. Figure 8 shows closure times of electrocontact probes plotted as a function of axial position (z) and azimuthal location (ϕ). Time is measured from the moment of the detonator trigger. The earliest time of arrival of the liner at the measuring unit was 27.876 μs (z = 1 mm, f = 300), the latest time of arrival was 28.274 μs (z = 19 mm, ϕ = 0). Maximum difference in time of probes closure (over both axial and radial coordinates) was 0.398 μs.

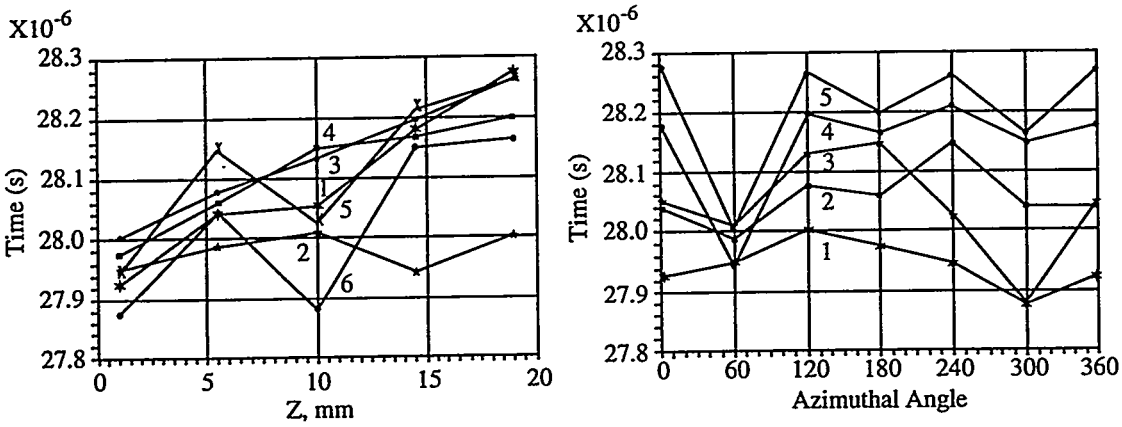

(a) (b)

Fig. 8. (a) Time of arrival as a function of axial position indicated by contact pins in the central measuring unit, lines connect probe at the same azimuth; (b) time of arrival as a function of azimuth indicated by contact probes, lines connect probes at same Z.

Figure 8 shows that upon arrival at the measuring unit, the liner had a conic shape. The part of the liner that arrived soonest was near the upstream electrode. In assembling the liner, the contact between the liner and the upstream electrode was made by thermal expansion of a brass ring, initially cooled to liquid nitrogen temperature. Upon warming, the ring expands and clamps the lower end of the liner assembly to the upstream electrode making a very good contact. Similarly, the data in Fig. 8 show an azimuthal asymmetry characteristic of a localized breakdown in the transmission line discussed earlier.

VII. RESULTS

Preshot calculations did not include the effect of the partial transmission line failure. Using the analysis above, we determined the approximate location of the transmission line failure. Modeling the failure as an inductive shunt applied across the line at the appropriate time, the current derivative in Fig. 9 were obtained. A time shift was applied to roughly align the maximum negative excursion in current derivative resulting from the fuse opening. Remarkably good agreement was noted between the model and the experiment at the peak value of the generator current derivative before the fuse operation; at the peak negative excursion during fuse operation (and subsequent closing of the load isolating switch), and at the first peak positive value of the current derivative after the closure of the crowbar switch. Some significant differences are noted in the current derivative at times prior to the first peak, and these were attributed to differences between the assumed and actual profile of the DEMG cavities. Significant differences are also noted at late times—well after the formation of the transmission line short. The discontinuity analysis applies immediately after the shunt current path forms and assumes a lossless, inductive shunt. The late time differences between model and experiment in Fig. 9 can be attributed to a substantial change in shunt impedance with time as large currents flow throughout the shunt.

After the system was completely assembled, it was possible to accurately measure all relevant dimensions, and a more accurate, "as built" characterization of the fuse, transmission line, diagnostic cavities, radial feed, and load were found. When these adjustments are made, the current derivative in the generator was recalculated as shown in Fig. 10. In the figure, the measured generator current derivative from the Δ ring and the calculated derivative are shown to correspond closely. Not only do the timing and magnitude of the maximum (prior to fuse operation) correspond accurately, but relatively small features during the generator run correspond as well. For example, the small feature in the calculation around 16 μs (resulting from the arrival on the symmetry plane of one of the corners in the generator cavity) is seen to correspond to a similar (though less distinct) feature in the experiment. In the experiment, small differences in timing and performance between cavities could be expected to lead to substantial smoothing of the current derivative.

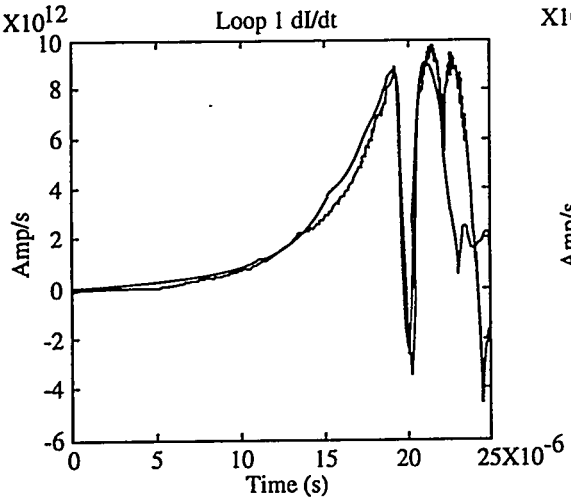

Fig. 9. Comparison of Δ Ring inductive probe data with preshot calculation using the "estimated" generator profile and shunt inductance.

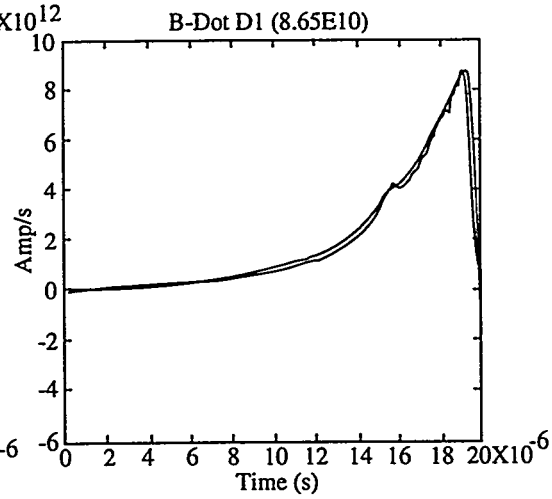

Fig. 10. Comparison of measured and calculated system performance.

With the results in Fig. 10, we can have reasonable confidence in the adequacy of current DEMG models. Systems using fuse opening switches and dynamic loads can likewise be adequately modeled.

REFERENCES

1. V. K. Chrenyshev *et al.*, "Results of Russian/US High Performance DEMG Experiment," *Proceedings of the 3rd International Conference on Megagauss Fields and Applications*, Novosibirsk, Russia (1983).

2. A. I. Petrukhin *et al.*, "Results of Russian/US High Performance DEMG Experiment," *Proceedings of the 5th International Conference on Megagauss Fields and Applications*, Novosibirsk, Russia (1989).

3. R. E. Reinovsky, I. R. Lindemuth, S. P. Marsh, and E. A. Lopez, "Explosive Pulse Power for Fusion Applications," *Proceedings of the 6th International Conference on Megagauss Fields and Applications*, Albuquerque, NM (1992).

4. R. E. Reinovsky and I. R.Lindemuth, "Design Consideration for 100 MJ Class Flux Compression Pulse Power Systems," *Proceedings of the 9th IEEE International Pulsed Power Conference*, Albuquerque, NM (1993).

5. I. R. Lindemuth, R. E. Reinovsky, and J. H. Goforth, "Exploding Metallic Fail Fuse Modeling at Los Alamos," *Megagauss Fields and Pulsed Power System* s, NOVA, p. 269 (1990).

6. VNIIEF Pre-Shot Report.